The Polar Resolver Using Pulse Technique

The Polar Resolver using Pulse Technique

Tadanori YONETANI*, Suemitsu MINAMOTO* and Kazuo MIYAKOSHI*

(Received June 15, 1971)

This paper deals with a polar resolver of 2-dimensional vectors. In general, for determining the magnitude and angle of the resultant vector when the vector quantities along the X, Y coordinate axes are given, several nonlinear computing elements, such as a sine- and a cosine-generators, multipliers and an automatic-gain-controlled amplifier, are indispensable. While using such nonlinear elements in order to solve the trigonometric problems, it is ordinarily difficult to obtain satisfactory accuracies at a little expense.

The polar resolver using pulse technique treated in this paper can be easily constructed with choppers and several IC's and brings us the answers of higher accuracies.

This paper describes its principles, error analyses and experimental results, in detail, and shows that the proposed resolver is applicable to the low speed analog computations of vector problems from its accuracies and frequency characteristics.

1. Introduction

The trigonometric transformations are normally classified into two types: polar to rectangular, and rectangular to polar. The authors have described the method of the former transformation in the previous paper[1]. We deal with the circuit for the latter transformation in this paper. In general, the rectangular-to-polar transformation is performed by utilizing sine- and cosine-generators, multipliers and an automatic-gain-controlled amplifier but it requires a great expense to use such nonlinear computing elements and we can hardly get the answers of required high accuracy. A new polar resolver using pulse technique is presented in this paper. From the results of error analyses and experimental research on the proposed resolver, it has become evident that the more accurate answers are obtainable by this resolver constructed with several fundamental circuits.

In this method, there lies the upper limit of the input signal frequency due to the sampling of the input signal in the process of generating the amplitude-modulated pulses. The results of spectral analyses show that the allowable frequency of the input signal is less than one half of the sampling frequency and that the static errors depend principally on the characteristics of the band-pass filter used in this resolver and may be decreased according to the quality of the filter. The resolver in the experiments has the accuracy of $\pm 0.2\%$ and the frequency range of input signal is from DC to 80 Hz for sampling frequency of 2.5 kHz.

2. Priciples of Operations

The rectangular-to-polar, or simply the "polar", transformation arises when the

* Department of Electronics, College of Engineering.

vector quantities A, B, along the X, Y coordinate axes are known and it is necessary to determine the magnitude R and angle θ of the resultant vector $\boldsymbol{R}$. The problem is identical to finding

$$R=\sqrt{A^2+B^2} \tag{1}$$

$$\theta=\tan^{-1} B/A \tag{2}$$

as in Fig. 1.

Now, we describe the circuit for finding the quantities R and θ given by Eqs. (1) and (2). Fig. 2 shows the block diagram of the proposed polar resolver and Fig. 3 the waveforms of circuits of the block diagram.

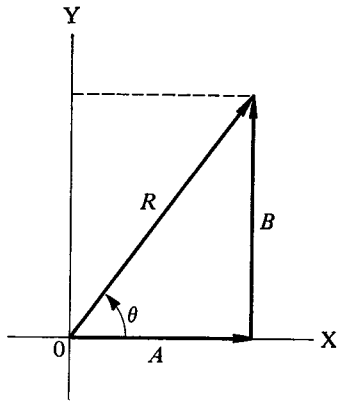

Fig. 1. Geometry of the rectangular-to-polar transformation.

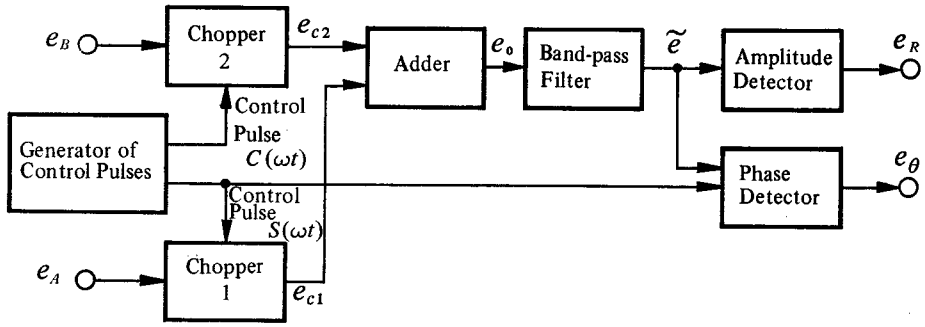

Fig. 2. Block diagram of the polar resolver.

The generator of control pulses in Fig. 2 generates the control pulses v_{c1} and v_{c2} of the fundamental angular frequency ω shown in Fig. 3 (a) and (b). The pulse v_{c2} leads the pulse v_{c1} exactly $\frac{1}{2}\pi$ in phase and they are expressed by Eqs. (3) and (4).

$$v_{c1}=V_c\cdot S(\omega t) \tag{3}$$

$$v_{c2}=V_c\cdot C(\omega t) \tag{4}$$

where

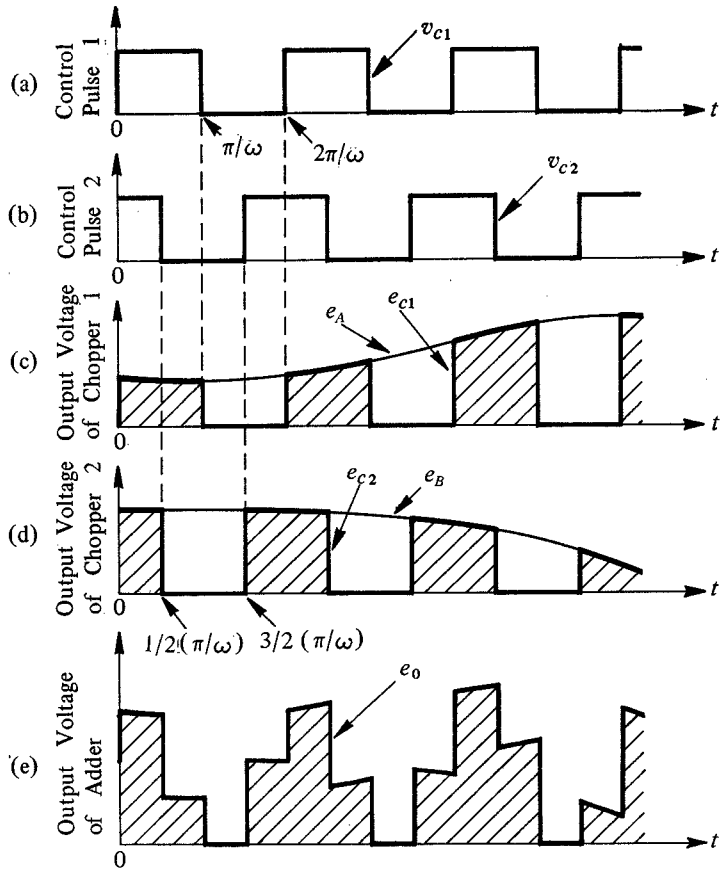

Fig. 3. Waveforms of circuits shown in Fig. 2.

$$S(\omega t)=\frac{1}{2}+\frac{2}{\pi}\sum_{l=1}^{\infty}\frac{\sin(2l-1)\omega t}{2l-1} \tag{3'}$$

$$C(\omega t)=\frac{1}{2}-\frac{2}{\pi}\sum_{l=1}^{\infty}(-1)\frac{\cos(2l-1)\omega t}{2l-1} \tag{4'}$$

V_c : the amplitude of control pulse v_{c1} or v_{c2}

In Fig. 2, the input signals e_A and e_B corresponding to A and B are applied respectively to the choppers 1 and 2 which are driven by the control pulses v_{c1} and v_{c2}. And then the output voltages e_{c1} and e_{c2} of choppers 1 and 2 shown in Fig. 3 (c) and (d) can be given as

$$e_{c1}=e_A S(\omega t)=e_A\left\{\frac{1}{2}+\frac{2}{\pi}\sum_{l=1}^{\infty}\frac{\sin(2l-1)\omega t}{2l-1}\right\} \tag{5}$$

$$e_{c2}=e_A C(\omega t)=e_A\left\{\frac{1}{2}-\frac{2}{\pi}\sum_{l=1}^{\infty}(-1)\frac{\cos(2l-1)\omega t}{2l-1}\right\} \tag{6}$$

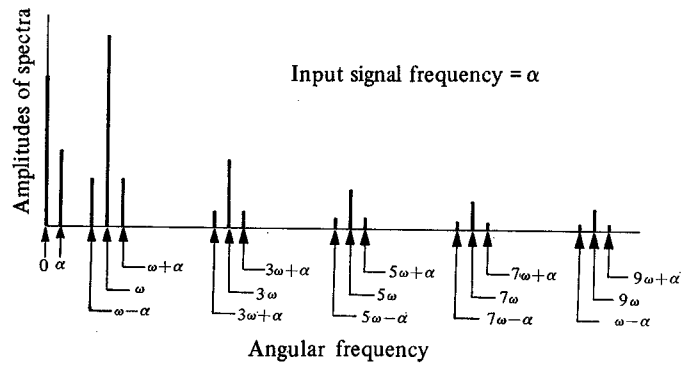

Fig. 4. Spectral distribution of output voltage of chopper.

Fig. 4 shows the spectral distribution of Eq. (5) in the case that the input signal frequency α is lower than $\frac{1}{2}\omega$. In Fig. 4, spectra of ω and $\omega \pm \alpha$ are required for the correct output signal and all of the others are unwanted. From Fig. 2, the output voltage of adder e_0 is given by

$$e_0 = e_{c1} + e_{c2} = e_A S(\omega t) + e_B C(\omega t) \tag{7}$$

By substituting Eqs. (3) and (4) into Eq. (7), Eq. (8) is obtained.

$$\begin{aligned} e_0 = {} & \frac{1}{2}(e_A + e_B) \\ & + \frac{2}{\pi}\sqrt{e_A^2 + e_B^2}\,\sin(\omega t + \tan^{-1} e_B/e_A) \\ & + \frac{2}{\pi}\sqrt{e_A^2 + e_B^2}\sum_{l=2}^{\infty}\frac{\sin\{(2l-1)\omega t + \theta_{2l-1}\}}{2l-1} \end{aligned} \tag{8}$$

where $\theta_{2l-1} = (-1)^{l+1}\tan^{-1} e_B/e_A$

The band-pass filter is for passing the signal spectra of ω and $\omega \pm \alpha$ expressed by Eq. (8) and for eliminating the unwanted ones except ω and $\omega \pm \alpha$. The ideal pass-band of the band-pass filter is $\pm\frac{1}{2}\omega$ centered at ω. Therefore, the output voltage e of the ideal band-pass filter is given by Eq. (9).

$$e = \frac{2}{\pi}\sqrt{e_A^2 + e_B^2}\,\sin(\omega t + \tan^{-1} e_B/e_A) \tag{9}$$

As the amplitude and phase angle in Eq. (9) are equivalent to Eqs. (1) and (2), the vector quantities R and θ in polar form can be found by detecting the amplitude $\frac{2}{\pi}\sqrt{e_A^2 + e_B^2}$ and phase angle $\tan^{-1} e_B/e_A$ of the sinusoidal wave given by Eq. (9). By means of an amplitude detector and a phase detector, the output signals proportional to the amplitude $\frac{2}{\pi}\sqrt{e_A^2 + e_B^2}$ and phase angle $\tan^{-1} e_B/e_A$ can be obtained from the output voltage e of band-pass filter. As the output voltage of the amplitude detector we can obtain the

signal voltage e_R given by

$$e_R = \frac{1}{2\pi}\int_0^{2\pi} |e|\, d(\omega t)$$
$$= \frac{4}{\pi^2}\sqrt{e_A{}^2 + e_B{}^2} \tag{10}$$

3. Error Analyses

Considerable factors which cause static errors are as follows:

(1) Offset voltages and drift voltages of the amplifiers used in the resolver
(2) Errors of the resistances and capacitances
(3) The unwanted spectra (higher harmonics of ω) remaining barely in the output voltage of band-pass filter though they are to be attenuated by using it

Of these factors, the unwanted spectra have fundamentally heavy influences upon the static errors of the resolver and the factors (1) and (2) may be neglected. Therefore we analyse the static errors due to the unwanted spectra theoretically in relation to the characteristics of the practical band-pass filter.

In the analyses of static errors, we may consider the input signals e_A and e_B to be nonperiodic voltages and e_A and e_B written as

$$e_A = \text{const.} \tag{11}$$

$$e_B = \text{const.} \tag{12}$$

And the output voltages e_p of the practical band-pass filter (center frequency: ω) is given by

$$e_p = \frac{2}{\pi}\sqrt{e_A{}^2 + e_B{}^2}\sin(\omega t + \tan^{-1} e_B/e_A)$$
$$+ \frac{2}{\pi}\sqrt{e_A{}^2 + e_B{}^2}\sum_{l=1}^{\infty}\frac{a_{2l-1}}{2l-1}$$
$$\times \sin\{(2l-1)\omega t + \theta_{2l-1} + \phi_{2l-1}\} \tag{13}$$

where $\theta_{2l-1} = (-1)^{l+1}\tan^{-1} e_B/e_A$

a_{2l-1} : the gain of the practical band-pass filter at $(2l-1)\omega$

ϕ_{2l-1} : the phase shift by the practical band-pass filter at $(2l-1)\omega$

This output voltage e_p is applied to the amplitude detector and phase detector. If the band-pass filter is designed that

$$a_1 \gg a_3 > a_5 > a_7 > \cdots > a_{2l-1} > \cdots$$

the output voltage e_{R_p} of the amplitude detector is given by

$$e_{R_p}=\frac{1}{2\pi}\int_0^{2\pi}|e_p|\,d(\omega t)$$
$$=\frac{4}{\pi^2}\sqrt{e_A{}^2+e_B{}^2}\left[1+\sum_{l=1}^{\infty}\frac{a_{2l-1}}{(2l-1)^2}\right.$$
$$\left.\times\cos\{-(2l-1)\tan^{-1}e_B/e_A+\theta_{2l-1}+\phi_{2l-1}\}\right] \tag{14}$$

where $\theta_{2l-1}=(-1)^{l+1}\tan^{-1}e_B/e_A$

The static error ε_R in the output signal of the amplitude detector can expressed by

$$\varepsilon_R=\frac{e_{R_p}-e_R}{\text{Full scale of } e_R} \tag{15}$$

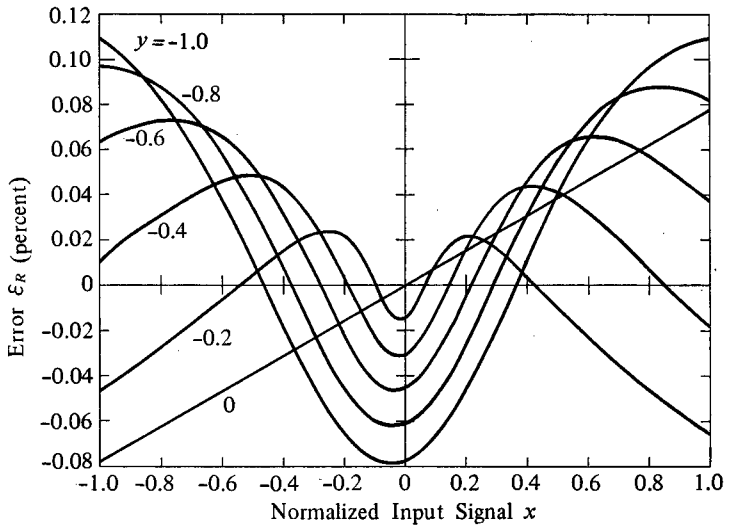

(a)

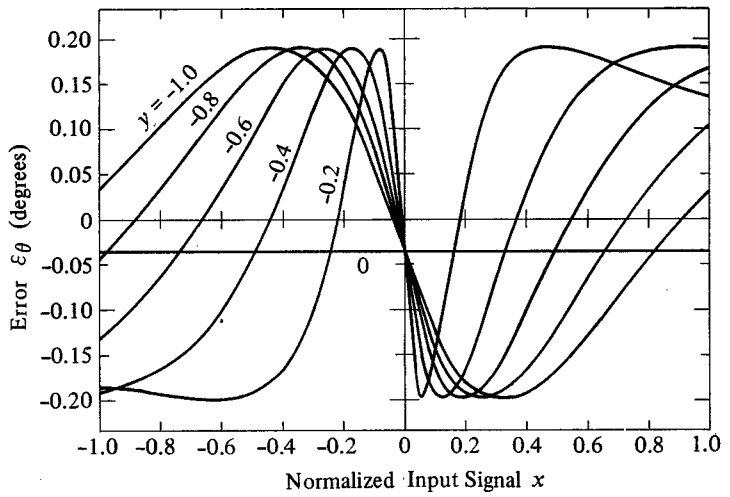

(b)

Fig. 5(a). Error curves (calculated) I.
(b). Error curves (calculated) II.

Substituting Eqs. (10) and (14) into Eq. (15), the following equation is obtained.

$$\varepsilon_R = \sqrt{x^2+y^2} \sum_{l=1}^{\infty} \frac{a_{2l-1}}{(2l-1)^2} \times \cos[-\{(2l-1)+(-1)^l\} \tan^{-1} y/x + \phi_{2l-1}] \tag{16}$$

where x, y : the input signals normalized with respect to their maximum values

Similarly we can find the static error ε_θ in the output signal of phase detector as follows:

$$\varepsilon_\theta \simeq \sum_{l=1}^{\infty} \frac{a_{2l-1}}{2l-1} \times \sin[-\{(2l-1)+(-1)^l\} \tan^{-1} y/x + \phi_{2l-1}] \tag{17}$$

Therefore the band-pass filter must be designed that the maximum values of Eqs. (16) and (17) may be less than the allowable levels.

For examples, the band-pass filter in the experiments is so designed that the calculated values of the static errors ε_R may be within $\pm 0.1\%$ and ε_θ be within ± 0.2 degrees as shown in Fig. 5 (a) and (b).

4. Analysis of Frequency Characteristics

When the input signal varies periodically, the frequency spectra centered at ω and its higher harmonics arise in the output voltage of chopper as shown in Fig. 4 and from this figure it is adequate that the frequency of input signal should be less than $\frac{1}{2}\omega$ and the ideal pass-band of the filter is $\pm\frac{1}{2}\omega$ centered at ω. If, within the pass-band, the gain of the filter is regarded to be sufficiently flat and the phase shift caused by it is negligible under the ideal conditions mentioned above, any distortion or error does not arise in its output signal. Therefore the highest frequency permitted to the input signal can be considered fundamentally to be $\frac{1}{2}\omega$. But, in practical cases, it is uneasy that, for the band-pass filter, the ideal qualities are assured over its pass-band.

Now, for practical cases, we define that its gain a and phase shift ϕ are as Eqs. (18) and (19).

$$a = g(\omega_i - \omega) \tag{18}$$

$$\phi = f(\omega_i - \omega) \tag{19}$$

where ω_i : the input signal frequency of the filter

ω : the center frequency of the filter (=the sampling frequency of choppers)

Now, leave the unwanted spectra in e_{c1} out of account for the sake of convenience and we can express the filter output e_{p1} corresponding to e_{c1} as follows:

$$e_{p1} = \frac{E_A}{\pi}\left[\sin\omega t + \frac{M}{2} g(-\alpha) \cos\{(\omega-\alpha)t + f(-\alpha)\} - \frac{M}{2} g(\alpha) \cos\{(\omega+\alpha)t + f(\alpha)\}\right] \tag{20}$$

where $0<M\leq 1$

It is adequate to the practical cases to assume that

$$g(\alpha)=g(-\alpha) \tag{18'}$$

$$f(\alpha)=-f(-\alpha) \tag{19'}$$

where α : the input signal frequency of the resolver

Substituting Eqs. (18) and (19) into Eq. (20), the following equation is obtained.

$$e_{p_1}=\frac{E_A}{\pi}\left[1+Mg(\alpha)\sin\{\alpha t+f(\alpha)\}\right] \times\sin\omega t \tag{21}$$

It is clarified from Eq. (21) that the amplitude-and phase-distortions are determined in relation to the characteristics of the band-pass filter.

5. Experimental Results

5.1 Experimental circuits

The experiments were conducted with a trial model having the circuit configuration shown in Fig. 2. The circuits of the choppers, the band-pass filter and the phase detector have been shown in previous papers[1),2)], and the amplitude detector consists of the absolute value circuit[1)] and the low-pass filter[1)]. The generator circuit of control pulses is shown in Fig. 6.

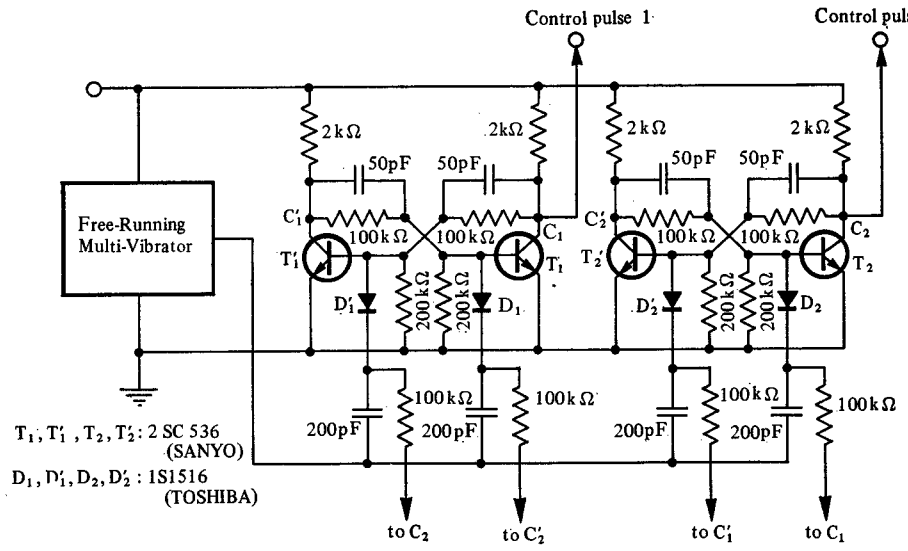

Fig. 6. Construction of the generator of control pulses.

5.2 Static characteristics and frequency response

Specifications of the trial model are as follows:

(1) e_A, e_B : ± 5V
(2) e_R : 10V
(3) e_θ : ± 9V($\pm 180°$)

Static characteristics of the experimental circuit are shown in Fig. 7 (a), (b) and the measured values in these figures are based on the records by X-Y recorder and the figures state

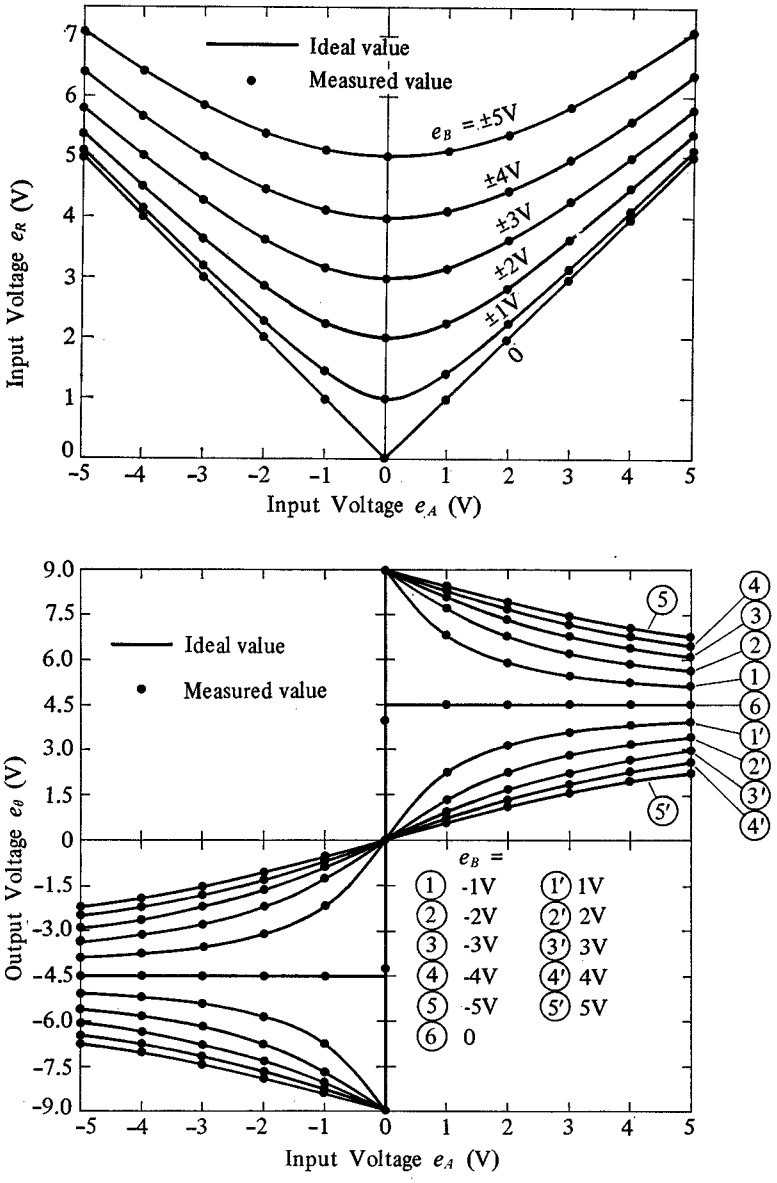

Fig. 7(a). Transfer characteristics of the resolver I.
(b). Transfer characteristics of the resolver II.

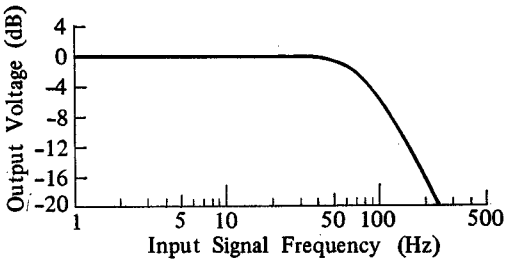

Fig. 8. Frequency characteristics of the resolvaer.

that the experimental circuit has the accuracy better than $\pm 0.2\%$ of full scale. The frequency response of the resolver is shown in Fig. 8.

6. Conclusions

From the error analyses and experimental results it can be suggested that the four-quadrant operation of the proposed resolver can be performed with relatively high accuracies. The resolver has a relatively simple construction of several fundamenal circuit blocks.

Hence, it is applicable to the low-speed analog computations or simulations which require accurate answers to trigonometric problems.

References

1) T. Yonetani, M. Daijo, S. Minamoto and K. Miyakoshi, Bull. of Univ. of Osaka Pref., A **18** 1 (1969).
2) T. Yonetani, S. Minamoto and K. Miyakoshi, Transactions of IECE of Japan, **52**-C, No. 3 (1967).